INFORMATICS JOURNALS

Research Article

Journal of Natural Remedies
DOI: 10.18311/jnr/2026/54097

eISSN:2320-3358|Vol26(4),2026|pp. 1051–1064

Anti-hyperlipidemic Potential of *Solonum nigrum*: Extraction, GC-MS Profiling, *In Silico* and *In Vivo* Evaluation

Vijaykumar Meti[1], Syed Atif Abbas[2], Imam Shaik[3], Anandarajagopal Kalusalingam[4], Syeda Zuleqaunnisa Begum[5], Ashok Kumar Uppuluru[6], Roohi Jamal[7], Faizan Sayeed[8], T. Shekeshavali[9], Mohammed Jaffer Sadik[10] and B. Tazneem[5*]

[1]Department of Pharmaceutics, KLE College of Pharmacy, Hubballi, Karnataka, India (A constituent Unit of KLE Academy of Higher Education and Research, Belagavi - 590010, Karnataka, India

[2]Faculty of Pharmacy, Quest International University, Ipoh - 30250, Perak, Malaysia

[3]Department of Pathology, School of Medicine, Taylor's University, No.1 Jalan Taylor's -47500, Subang Jaya, Malaysia

[4]School of Pharmacy, KPJ University, Nilai - 71800, Negeri Sembilan, Malaysia

[5]Deccan School of Pharmacy, Osmania University, Hyderabad - 500001, Telangana, India; btaspharm@gmail.com

[6]Max Institute of Pharmaceutical Sciences, Khammam - 507002, Telangana, India

[7]K B H S S trust's institute of Pharmacy, Bhaygon road, Malegaon, Nashik - 423105, Maharashtra, India

[8]MESCO College of Pharmacy, Hyderabad - 500006, Telangana, India

[9]National College of Pharmacy, Shimoga - 577201, Karnataka, India

[10]Sri Indu Institute of Pharmacy, Sheriguda, Hyderabad - 501510, Telangana, India

Abstract

Aim: This study aimed to evaluate the anti-hyperlipidemic potential of the ethyl acetate fraction of whole *Solonum nigrum* (*S. nigrum).* The objective of this study was to perform GC-MS profiling of the extract and in silico (molecular docking and ADMET) analyses of the identified constituents. **Methods:** Dried whole-plant powder of *S. nigrum* was extracted using a Soxhlet apparatus with ethyl acetate. GC-MS analysis of the obtained extract was performed to identify its constituents. Subsequently, *in silico* (molecular docking and ADMET) analyses of the identified constituents were performed. This was followed by the determination of *the in vivo* anti-hyperlipidemic activity of the extract (100, 200, and 300 mg/kg) against Triton X-100-induced hyperlipidemia in rats. Parameters such as body weight, blood glucose level, and lipid profile were also evaluated. This was followed by histopathological analysis of the heart and liver tissues. Statistical significance was set at $p<0.05$. **Results:** The percentage yield of the ethyl acetate fraction of *S. nigrum* was 0.6% and was rich in flavonoids, glycosides, saponins, carbohydrates, alkaloids, and proteins. GC-MS analysis identified 10 constituents, among which the major were ethane (70.64%), 1-chloro-1-fluoro (0.94%), and undecanoic acid (0.86%). Molecular docking studies showed that phytol exhibited a binding affinity comparable to that of Fluvastatin. ADMET analysis revealed that most of the identified

(Article Chronicle: Article Received on: 17.12.2025; Revised on: 23.02.2026; Accepted on: 16.03.2026)

*Author for correspondence

constituents had a favourable pharmacokinetic profile, with minimal violation of Lipinski's rule of 5. In both Triton X-100-induced hyperlipidemic rats, *S. nigrum* at all doses significantly reduced the increase in body weight, normalised blood glucose levels, and improved lipid profiles. Histopathological analysis revealed restoration of the normal architecture of heart and liver tissue and minimal deposition of collagen fibre in both tissues, specifically at higher doses of the test extract. **Conclusion:** The *S. nigrum* demonstrated hypolipidemic effect against Triton X- 100 induced hyperlipidemia in rats, significantly reducing body weight, glucose, and normalising lipid profile. These findings suggest that *S. nigrum*, specifically its phytol content, may serve as a potential herbal drug for managing hyperlipidemia and associated metabolic disorders.

Major Findings: The ethyl acetate fraction of the whole plant of *S. nigrum* exhibited significant anti-hyperlipidemic effects against Triton X- 100 induced hyperlipidemia in rats. Phytol may be the contributing compound responsible for the antihyperlipidemic effect of the extract.

Keywords: GCMS, Hyperlipidaemias, Molecular Docking, Phytol, *Solanum nigrum*

1. Introduction

Hyperlipidemia is characterised by increased levels of cholesterol, triglycerides (TGs), or both[1]. This metabolic disorder is categorised based on the type of lipid that is elevated and patterns of inheritance[2]. It is broadly divided into primary and secondary types. Primary hyperlipidemia encompasses isolated cholesterol elevation, isolated TG elevations, or both, as mentioned above, and the main causes of this type include genetic factors, environmental influences, or a combination of both. Secondary hyperlipidemia, on the other hand, results from factors such as medications, dietary habits or underlying medical conditions[3].

Hyperlipidemia is a recognised metabolic abnormality that increases the risk of atherosclerosis and diseases affecting the cardiovascular, cerebrovascular, and peripheral vascular systems[4]. Each year, approximately 17 million individuals worldwide succumb to Cardiovascular Disease (CVD), with hyperlipidemia being the most significant attributable risk factor[5]. These findings have led to recent efforts promoting the prevention and management of hyperlipidemia as a crucial risk factor, emphasising its prognostic importance in reducing the incidence of stroke and Myocardial Infarction (MI)[6].

Treating hyperlipidemia primarily involves consistently lowering lipid levels through various medications such as statins, fibrates, bile acid sequestrants, and niacin. However, the effectiveness of these drugs is debatable due to their numerous side effects[7]. Recent investigation into medicinal herbs and dietary supplements used in traditional medicine indicates that their components, including dietary fibres, vitamins, flavonoids, sterols and other antioxidants, can reduce lipids, prevent LDL oxidation, and neutralise oxygen-free radicals. Consequently, they are beneficial in treating this condition by influencing the immune system and enhancing the body's metabolic functions[8].

Solanum nigrum L., commonly known as Black Nightshade in English, is a member of the Solanaceae. Originally native to Europe, Asia, and North America, it has spread to South America, Australia, and Africa. This plant is widely distributed across tropical and temperate regions, representing one of the most diverse and variable species groups within its genus[9]. *S. nigrum* has been reported to be rich in glycoalkaloids, including solanine, solamargine, and solasodine. Additionally, various flavonoids have been identified, such as quercetin, luteolin, malvidin, pelargonidin, rutin, naringenin, apigenin, and kaempferol. Other components found in the plant include carbohydrates, saponins, and sterols[10]. *S. nigrum* has a wide range of therapeutic applications. These include its ability to clear heat, remove toxins, reduce swelling and lumps, as well as its anti-inflammatory and diuretic effects. The plant is also known to stimulate saliva production and alleviate thirst. In Indian ayurvedic medicine, *S. nigrum* has been utilised to treat various conditions, including intestinal disease, ulcers, diarrhoea, and skin disorders. Scientifically, it has been proven to have anti-cancer, anti-tumour, anti-inflammatory, anti-oxidant, and antihypertensive properties[11].

Given its established therapeutic effects and medicinally significant chemical profile, the present study focuses on exploring the anti-hyperlipidaemic potential of *S. nigrum*. This study encompasses several

objectives, such as the extraction of the whole plant of *S. nigrum*, performing GC-MS analysis to identify the extract's chemical profile, conducting computational studies (molecular docking and ADMET analysis), and assessing the extract's anti-hyperlipidemic potential against *in vivo* Triton X-100 induced hyperlipidemia.

2. Materials and Methods

2.1 Chemicals

Triton X- 100, S.D. Fine, Mumbai, India and atorvastatin, a gift sample from Nuwill research and innovation Pvt. Ltd., Bangalore, kit was purchased from Erba diagnostics Mannheim GmbH, India.

2.2 Plant Material

The whole plant of *S. nigrum* was identified and collected from the local area of Hyderabad. The sample was authenticated by Dr A. Vijay Bhasker Reddy, Assistant Professor, Department of Botany, Osmania University, Hyderabad, who identified the plant and a specimen was deposited at Deccan School of Pharmacy (Voucher no.OUAS-235).

2.3 Experimental Animals

Wistar albino rats of male, 9-11 weeks old, weighing 160-180 g, weighing were used for the study. The animals were purchased from Mahaveera Enterprises in Hyderabad and housed under standard conditions of temperature (25 ± 2°C), humidity (45-55%) and light (12h light/12 h dark). The rats were given standard food pellets and water *ad libitum*. The experimental protocol was designed as per the CPCSEA guidelines and approved by IAEC HKES's MTRIPS under protocol number MTRIPS/IAEC/143/2022-23.

2.4 Extraction of Plant Material

The whole plant of *S. nigrum* was dried in the shade and pulverised into fine powder. 150 g of dried powder was sequentially extracted with 250 ml of solvent of increasing polarity (hexane, chloroform, ethyl acetate and n-butanol) using a Soxhlet apparatus. The temperature was maintained in the range of 20-30 °C for ethyl acetate. The extraction process continued till the colour in the siphon became clear (approximately 6 hours), and the dark colour extracted was collected in the round-bottom flask. The resulting ethyl acetate extract was evaporated under vacuum by a rotary evaporator[12]. Afterwards, the percentage yield of the ethyl acetate extract was calculated, and phytochemical screening was done[13].

2.5 GC-MS Analysis

For qualitative GC-MS analysis, a Shimadzu GC-MS (QP2010) gas chromatograph-mass spectrometer with a Shimadzu auto-injector AOC-20 was employed. The GC-MS Lab Solution software from Shimadzu was used for data acquisition. The injector was set to 260°C, while the oven temperature was programmed to start at 60°C for 2 min, then increase by 10°C/min to 300°C, and hold for 6 min. A Supel co-wax column (30 mm X 0.25 mm i.d. 0.25 µm film thickness) from Merck was used. The GC-MS featured a split-spitless injector at 260°C, with a 0.4 µL injection volume in split mode (10:1 ratio). The inlet pressure was 37.7 kPa, and helium served as the carrier gas at a constant linear velocity of 30 cm/s. The interface temperature was kept at 250°C. The MS operated with electron ionisation, using a 0.95 kV detector voltage and a mass range of 40 to 350 u. Scans were performed at 1666 amu per second with a 0.20-second interval. Ethyl acetate fractions were identified by comparing their mass spectra with those in the Mass Spectral Database (FFSNC 2, NIST 11, Wiley 9) and Retention Indices (RI). These indices were calculated relative to the retention times of a series of n-hydrocarbons (C7-C30) and compared with values reported in the literature.

2.6 *In Silico* Investigation: Molecular Docking and ADMET Analysis

The three-dimensional structure of the target protein (HMG-CoA reductase, PDB ID: 1HWI) was retrieved from the Protein Data Bank (PDB). The ligand (phytoconstituents identified by GC-MS) was obtained from the PubChem database. Ligand preparation, including energy minimisation (RMSD cut-off 1.5 Angstrom) and 3D structure optimisation, was performed using LigPrep (Schrodinger, LLC). Molecular docking was performed using Glide (Schrodinger, LLC, version 9.1, New York). A grid representing the protein's binding region was established (Grid parameter: inner box 10 x 10 x 10 angstrom and outer box 20 x 20 x 20 Angstrom).

Docking was carried out in Standard Precision mode. Subsequently, docking scores and binding energy (ΔG) were evaluated to assess the strength of ligand-protein interactions. Pharmacokinetic properties and toxicity of the compounds were assessed using ADMET analysis before experimental validation[14-16].

2.7 *In Vivo* Anti-hyperlipidaemic Activity Evaluation

2.7.1 Selection of Dose

To carry out further *in vivo* activity, three doses of *S. nigrum* extract were selected: 100, 200 and 300 mg/kg BW, based on previous literature[17,18].

2.7.2 Anti-hyperlipidaemic Activity of S. nigrum Extract Against Triton X- 100 X- 100 Induced Hyperlipidemia

Wister rats were divided into 6 groups containing 6 rats in each group (n=6). Afterwards, the rats were kept fasting for 24 h. After the fasting period was over, the rats were injected with a single dose of saline solution of Triton X- 100 (200 mg/kg, i.p). After 48 hrs of the Triton X- 100 injection, the experimental groups received their respective treatment for seven days as follow: Group I: Normal control: received normal saline 10 ml/kg/day, p.o.; Group-II: Negative control: received single dose of Triton X- 100 X- 100 (200 mg/kg, i.p); Group-III: Standard: received single dose of Triton X- 100 (200 mg/kg, i.p) + Atorvastatin (8 mg/kg p.o.); Group-IV: Test: received single dose of Triton X-100 (200 mg/kg, i.p) + EA SN 100 mg/kg p.o; Group-V: Test: received single dose of Triton X- 100 (200 mg/kg, i.p) + EA SN 200 mg/kg p.o.; Group-VI: Test: received single dose of Triton X- 100 (200 mg/kg, i.p) + EA SN 300 mg/kg p.o. for seven days[19].

2.7.3 Parameters Estimated

Both initial and final body weight of Wistar albino rats were measured using an animal weighing scale (ATOM – A115C digital balance). Secondly, blood glucose level was determined using a blood glucometer (Dr Morepen). Finally, estimation of serum lipid levels was done. Under a little ether anaesthetic, blood was drawn through a retro-orbital sinus puncture. The collected samples were centrifuged for 10 minutes at 3000 rpm to obtain serum for analysis of Total Cholesterol (TC), Total Triglyceride (TG), High-Density Lipoprotein (HDL), Low-Density Lipoprotein (LDL) and Very Low-Density Lipoprotein (VLDL) using commercially available diagnostic kits (Erba Mannheim, Transasia Bio-Medicals Ltd., India).

2.7.4 Histopathological Analysis of Heart and Liver

Heart and liver tissues were isolated and kept in 10% neutral buffered formalin. The tissue samples underwent a dehydration process with ethanol, followed by xylene clearing, before paraffin wax embedding. For the purpose of evaluating overall tissue morphology, 4-5 µm thick sections were cut from the paraffin blocks utilising a microtome. These sections were then processed with Haematoxylin and Eosin (H and E) staining and Masson's Trichrome Stain (MTS) techniques[20,21].

2.8 Statistical Analysis

Data was analysed using GraphPad Prism version 8. Values are expressed as Mean ± SEM and analysed using one-way ANOVA followed by Dunnett's test of multiple comparisons. The criterion of statistical significance was $p<0.05$.

3. Results

3.1 Percentage Yield and Phytochemical Screening

The percentage yield of the ethyl acetate extract was found to be 0.6%, and the extract was found to be rich in flavonoids, glycosides, saponins, carbohydrates, alkaloids and protein.

3.2 GC-MS Analysis of the Ethyl Acetate Fraction of *S. nigrum*

GC-MS analysis of the whole plant ethyl acetate fraction of *S. nigrum* revealed the presence of Ethane, 1-chloro-1-fluoro- (26.01 and 70.64%), phytol (0.94%), undecanoic acid (0.86%), 1-Heptanol, 6-methyl- (0.40%) as the major constituents. 2-Propenoic acid, 2-methyl-,2-propenyl ester (0.34%), 1-Undecene, 9-methyl (0.29%), trifluoroacetic acid, n-tetradecyl ester (0.10%), 1-Heptanol, 2,4-dimethyl-, (R, R)-(+)- (0.06%), Cyclopentamethanol, a, alpha. – (1-methylethyl)-2-nitro (0.02%) as minor constituents (Table 1, Figure 1).

Table 1. Phytoconstituents identified in the ethyl acetate fraction of *S. nigrum*

Peak	Name	Area %	Match score
1	Ethane, 1-chloro-1-fluoro-	70.64	74
2	2-Propenoic acid, 2-methyl-,2-propenyl ester	0.34	72
3	1-Heptanol, 6-methyl-	0.40	79
4	1-Dodecene	0.37	84
5	Undecanoic acid	0.86	81
6	1-Undecene,9-methyl-	0.29	84
7	Phytol	0.94	86
8	Trifluoroacetic acid, n-tetradecyl ester	0.10	84
9	1-Heptanol, 2,4-dimethyl-, (R,R)-(+)-	0.06	76
10	Cyclopentamethanol, a alpha. –(1-methylethyl)-2-nitro	0.02	69

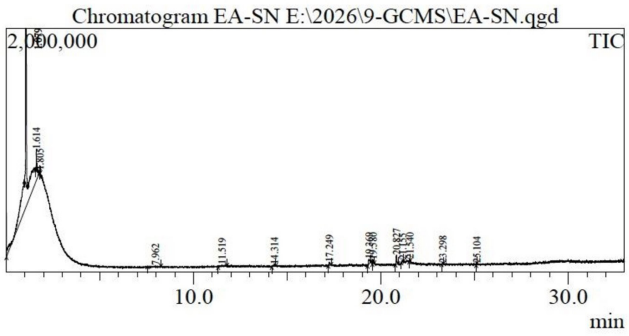


Figure 1. GC-MS chromatogram of the ethyl acetate fraction of *S. nigrum* whole plant.

3.3 Molecular Docking and ADMET Analysis

The molecular docking analysis reveals varying binding strength of the identified compound from *S. nigrum* in comparison to standard Fluvastatin, which exhibits strong binding to the receptor HMG-CoA reductase (PDB 1D: 1HWI) with a dock score of -3.760 and a DG bind of -42.49 kcal/mol. Among the identified constituents, Phytol shows the most promising interaction with a DG bind of -44.78 kcal/mol and a dock score of -1.381. While its dock score is lower than standard Fluvastatin, it demonstrated the most favourable binding energy among all test compounds. Trifluoroacetic acid, n-tetradecyl ester (DG bind: 31.94 kcal/mol, dock score: -0.349), Undecanoic acid (DG Bind: -26.03 kcal/mol, dock score 1.725) and 1-Undecene, 9-methyl-(DG bind: -33.02 kcal/mol, dock score: 2.284) exhibit weaker interaction compared to Fluvastatin. Other compounds, benzene, Ethane (1-chloro-1-fluoro), and 2-Propenoic acid, 2-methyl-, 2-propenyl ester, have dock scores near zero or positive values, indicating poor binding affinity. Results are shown in Table 2 and Figure 2.

The identified compounds from the ethyl acetate fraction of *S. nigrum* showed varying degrees of interaction with the active residue of HMG-CoA reductase (PDB 1D:1HWI), with Fluvastatin as the standard drug. Fluvastatin forms multiple hydrogen bonds with ARG590, SER684, LYS692, LYS691 and ASP690, along with a salt bridge with LYS692, showing stable interaction with bond length ranging between 1.74 – 2.93 Å. Ethane, 1-chloro-1-fluoro-, and benzene do not interact with the receptor. Phytol, on the other hand, forms two hydrogen bonds with ARG590 and ASP690 with bond lengths of 1.94 Å and 1.75 Å, respectively, indicating moderate binding affinity and stability with the receptor's active site. Similarly, Undecanoic acids form both hydrogen bonds (SER684) and salt bridge (ARG590, LYS692) with distances ranging from 1.71 Å to 3.91 Å, indicating moderate binding. Constituents such as 2-propenoic acid, 2-methyl-,2-propenyl ester, and 1-heptanol, 6-methyl-,

Table 2. Molecular docking analysis of constituents identified in the ethyl acetate fraction of *S. nigrum*

Compound name	Dock score	DG bind
Ethane, 1-chloro-1-fluoro-	-0.984	-13.64
2-Propenoic acid, 2-methyl-, 2-propenyl ester	0.705	-20.36
1-Heptanol, 6-methyl-	-0.487	-20.84
1-Dodecene	2.963	-39.63
Undecanoic acid	1.725	-26.03
1-Undecene, 9-methyl-	2.284	-33.02
Phytol	-1.381	-44.78
Trifluoroacetic acid, n-tetradecyl ester	-0.349	-31.94
1-Heptanol, 2,4-dimethyl-, (R,R)-(+)-	-0.721	-24.16
Cyclopentanemethanol, .alpha.-(1-methylethyl)-2-nitro-, [1.alpha.(s@),2.alpha.]-	-2.262	-25.28
Standard: Fluvastatin	-3.760	-42.49

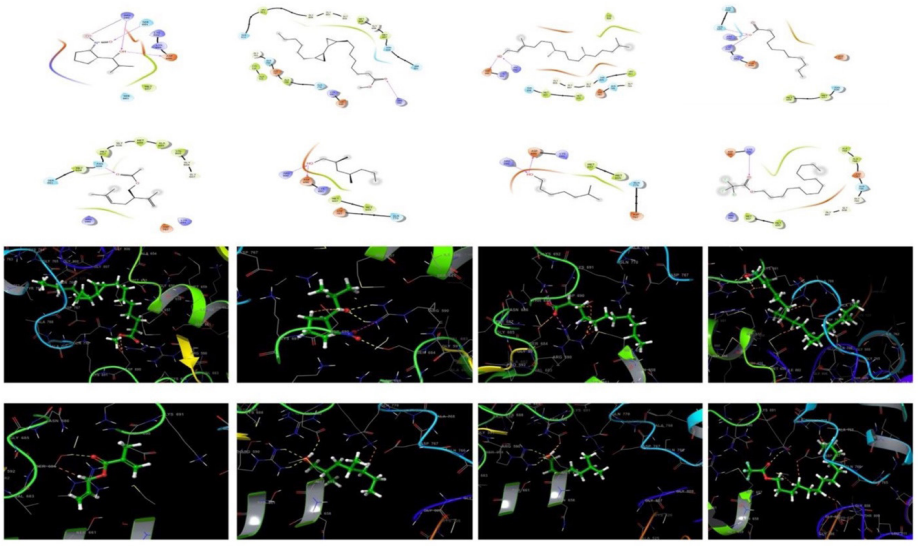


Figure 2. 2D and 3D structure of active bioactive compounds: **(a).** [1,1'-Bicyclopropyl]-2-octanoic acid, 2'-hexyl-, methyl ester; **(b).** Cyclopentanemethanol, .alpha.-(1-methylethyl)-2-nitro-, [1.alpha.,2.alpha.]-; **(c).** Undecanoic acid; **(d).** Phytol; **(e).** 2-Propenoic acid, 2-methyl-, 2-propenyl ester; **(f).** 1-Heptanol, 2,4-dimethyl-, (R, R)-(+)-; **(g).** 1-Heptanol, 6-methyl-; **(h).** Trifluoroacetic acid, n-tetradecyl ester.

form only one or two hydrogen bonds with residues SER684, ARG590, and ASP690, but a shorter range of interaction, suggesting weaker binding (Table 3).

The standard compound Fluvastatin has high GI absorption and fulfils Lipinski's rule of 5 with a synthetic accessibility score of 4.31. Ethane, 1-chloro-1-fluoro-, exhibited low MW and LogP, low GI absorption and no BBB permeability. Contrarily, 2-Propenoic acid, 2-methyl-,2-propenul ester, and 1-Heptanol,6-methyl- exhibited high GI absorption and BBB permeability. Undecenoic acid showed high GI absorption and no Lipinski violation. Phytol showed high LogP but not more than 5, low GI absorption, and lacks BBB permeability with a synthetic accessibility score of 4.30. However, none of the identified constituents had more than 1 violation of Lipinski's rule. Constituents, namely 1-Dodecene, phytol, trifluoroacetic acid, 1-Undecene,9-methyl, showed one violation of Lipinski's rule. The rest of the identified compounds exhibited zero violation of Lipinski's rule. Results are given in Table 4.

The toxicity profile of the identified compound was determined using Protox-II. Standard Fluvastatin was found to be safe as it is less active for hepatotoxicity, carcinogenicity and cytotoxicity and inactive for immunotoxicity and mutagenicity. Ethane, 1-chloro-1-fluoro- and phytol depicted low toxicity with most endpoints, including hepatotoxicity, immunotoxicity, mutagenicity, and cytotoxicity, depicted to be inactive or less active. Benzene was flagged as highly carcinogenic. Compounds such as 2-Propenoic acid,2-methyl-,2-propenyl ester, trifluoroacetic acid, and cyclopentanemethanol exhibited moderate toxicity, with some being less active for carcinogenicity or mutagenicity. The class in which these compound fall as per Protox-II is given in Table 5.

4. Effect of Ethyl Acetate Fraction of *S. nigrum* Against Triton X-100 X-induced Hyperlipidaemia

4.1 Body Weight (gm)

As seen in Figure 3, a significant increase in the body weight of Triton X-100-induced hyperlipidemic rats was observed compared to that of normal control rats ($p<0.0001$). Atorvastatin (AVS), EA SN 100, 200 and 300 mg/kg treated rats showed significantly reduced body weight to 181.12 ± 1.30, 201.24 ±1.42, 200.18 ± 0.93 and 198.08 ± 1.96 compared to 212.45 ± 0.99 in Triton X- 100 induced hyperlipidaemic rats ($p<0.0001$).

4.2 Blood Glucose Level (gm/dL)

A significantly higher blood glucose level (BGL) was observed in Triton X- 100 treated hyperlipidemic rats than in normal control rats ($p<0.0001$). AVS,

Table 3. Hydrogen bonding pattern of identified constituents from the ethyl acetate fraction of *S. nigrum*

Compound name	2D interaction	Distance
Ethane, 1-chloro-1-fluoro-	No interaction	No distance
2-Propenoic acid, 2-methyl-, 2-propenyl ester	H-bond:SER684	2.17
1-Heptanol, 6-methyl-	H-bond:ARG590,ASP690	2.13,1.57
1-Dodecene	No interaction	No distance
Undecanoic acid	H-bond:SER684 Salt-bridge:ARG590,LYS692	1.71 2.99,3.91
1-Undecene, 9-methyl-	No interaction	No distance
Phytol	H-bond:ARG590,ASP690	1.94,1.75
Trifluoroacetic acid, n-tetradecyl ester	H-bond: LYS691	2.13
1-Heptanol, 2,4-dimethyl-, (R,R)-(+)-	H-bond:ARG590,ASP690	1.89,1.90
Cyclopentanemethanol, .alpha.-(1-methylethyl)-2-nitro-, [1.alpha.(s@),2.alpha.]-	H-bond:ARG590,SER684,ASP690 Salt-bridge: ARG590	2.12,2.26,1.57 4.73
Fluvastatin	H-bond:ARG590,SER684,LYS692,LYS691, ASP690,ASP690 Salt-bridge: LYS692	1.74,2.01,2.35,2.69, 1.80,1.85 2.93

H-bond = Hydrogen bond; Salt-bridge = Ionic interaction between charged residues. Amino acid abbreviations: ARG = Arginine, ASP = Aspartic acid, LYS = Lysine, SER = Serine. All distances are in Angstroms (Å).

Table 4. ADME analysis of identified constituents from the ethyl acetate fraction of *S. nigrum*

Sr. no.	Compound Name	MW	H-bond Acceptor	H-bond Donors	Log P	GI Absorption	BBB Permeability	Bioavailability Score	Lipinski Violation	Synthetic Accessibility
1	Ethane, 1-chloro-1-fluoro-	82.50 g/mol	1	0	1.40	Low	No	0.55	0	1.38
2	2-Propenoic acid, 2-methyl-, 2-propenyl ester	126.15 g/mol	2	0	2.25	High	Yes	0.55	0	1.57
3	1-Heptanol, 6-methyl-	130.23 g/mol	1	1	2.46	High	Yes	0.55	0	1.44
4	1-Dodecene	168.32 g/mol	0	0	3.64	Low	No	0.55	1	2.16
5	Undecanoic acid	186.29 g/mol	2	1	2.74	High	Yes	0.85	0	1.77
6	1-Undecene, 9-methyl-	168.32 g/mol	0	0	3.52	Low	No	0.55	1	2.62
7	Phytol	296.53 g/mol	1	1	4.85	Low	No	0.55	1	4.30
8	Trifluoroacetic acid, n-tetradecyl ester	310.40 g/mol	5	0	4.66	Low	No	0.55	1	2.47
9	1-Heptanol, 2,4-dimethyl-, (R,R)-(+)-	144.25 g/mol	1	1	2.78	High	Yes	0.55	0	2.26
10	Cyclopentanemethanol, .alpha.-(1-methylethyl)-2-nitro-, [1.alpha.(s@),2.alpha.]-	187.24 g/mol	3	1	0.17	High	Yes	0.55	0	3.34
11	Fluvastatin	411.47 g/mol	5	3	2.62	High	No	0.56	0	4.31

Table 5. Toxicity prediction of identified compounds from *S. nigrum* using Protox-II

Name of the compound	ProTox-II Class	Hepatotoxicity	Carcinogenicity	Immunotoxicity	Mutagenicity	Cytotoxicity
Ethane, 1-chloro-1-fluoro-	5	Inactive	Inactive	Inactive	Inactive	Less Inactive
2-Propenoic acid, 2-methyl-, 2-propenyl ester	3	Inactive	Less Active	Inactive	Inactive	Inactive
1-Heptanol, 6-methyl-	4	Inactive	Less Inactive	Inactive	Inactive	Inactive
1-Dodecene	6	Inactive	Less Inactive	Inactive	Inactive	Inactive
Undecanoic acid	6	Less Inactive	Less Inactive	Inactive	Inactive	Inactive
1-Undecene, 9-methyl-	6	Inactive	Less Inactive	Inactive	Inactive	Inactive
Phytol	5	Inactive	Inactive	Inactive	Inactive	Inactive
Trifluoroacetic acid, n-tetradecyl ester	5	Inactive	Less Active	Inactive	Inactive	Inactive
1-Heptanol, 2,4-dimethyl-, (R,R)-(+)-	4	Inactive	Less Inactive	Inactive	Inactive	Inactive
Cyclopentanemethanol, .alpha.-(1-methylethyl)-2-nitro-, [1.alpha.(s@),2.alpha.]-	5	Less Inactive	Less Active	Inactive	Less Active	Inactive
Fluvastatin	4	Less Active	Less Inactive	Inactive	Inactive	Less Inactive

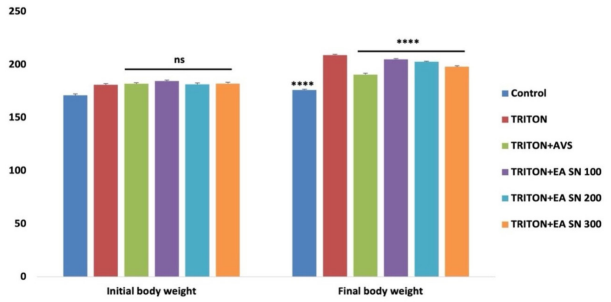


Figure 3. Effect of EA fraction of *S. nigrum* (EA SN) and atorvastatin (AVS) on body weight gain in Triton X-100- X induced hyperlipidemic rats.

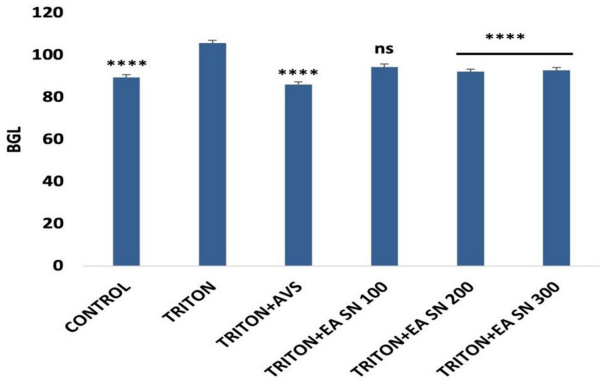


Figure 4. Effect of EA fraction of *S. nigrum* (EA SN) and atorvastatin (AVS) on Blood glucose level (gm/dl) in Triton X- 100 induced hyperlipidaemic rats.

EA SN200, and EA SN 300 mg/kg-treated rats had significantly reduced BGL compared to 85.70 ± 1.83, 92.60 ± 2.7, and 93.10 ± 1.09, respectively, compared to 105.94 ± 1.89 in Triton X-100-treated hyperlipidemic rats ($p<0.0001$). However, no significant reduction in BGL (94.50 ± 1.76) was found in EA SN100 mg/kg treated rats compared to Triton X- 100 X treated hyperlipidemic rats (Figure 4).

4.3 Lipid Profile

As shown in Figure 5, Triton X- 100 X induced group (negative control) showed elevated levels of TC, TG, LDL, VLDL and low levels of HDL compared to normal control ($p<0.0001$).

4.3.1 TC (mg/dL)

AVS, EA SN200 and EA SN300 treated rats significantly reduced TC level to 157.70 ± 1.97, 164.7 ± 2.0 and 160.30 ± 1.95, respectively, compared to 189.18 ± 2.04 in Triton X- 100 induced hyperlipidaemic rats ($p<0.0001$). On the other hand, EA SN100 treated rat also significantly reduced TC to 170.60 ± 2.02

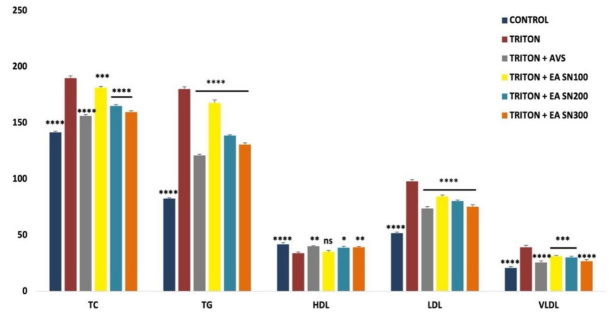


Figure 5. Lipid profile of various treatments against Triton X- 100 induced hyperlipidaemia.

compared to Triton X- 100 induced hyperlipidaemic rat ($p<0.001$).

4.3.2 TG (mg/dL)

AVS, EA SN100, EA SN200, and EA SN300 treated rats significantly reduced TG levels to 120.16 ± 2.50, 154.70 ± 2.02, 139.1±2.8 and 130.31± 2.24, respectively, compared to 180.14 ± 2.67 in Triton X- 100 induced hyperlipidaemic rats ($p<0.001$).

4.3.3 HDL (mg/dL)

AVS and EA SN300 treated rats showed significantly elevated HDL levels to 39.09 ±1.2 and 38.80 ± 0.90, respectively, compared to 35 ± 1.31 in Triton X- 100 induced hyperlipidaemic rats ($p<0.01$). EA SN200-treated rats showed a significant elevation in HDL level to 36.98 ± 0.86 compared to Triton X- 100 induced hyperlipidaemic rats ($p<0.05$). However, no significant difference in the same was found among EA SN 100 treated rats (39.09 ± 0.99) and Triton X- 100 X induced hyperlipidemic rats.

4.3.4 LDL (mg/dL)

AVS, EA SN100, EA SN200, and EA SN300 treated rats showed significantly reduced LDL levels to 75.81 ± 0.92, 84.97 ± 1.10, 80.5 ± 0.98 and 77.80 ± 1.03, respectively, compared to 97.21 ± 1.14 in Triton X- 100 induced hyperlipidaemic rats ($p<0.0001$).

4.3.5 VLDL (mg/dL)

AVS and EA SN300-treated rats depicted significantly reduced VLDL levels to 20.40 ± 0.65 and 29.02 ± 0.64, respectively, compared to 40.35 ± 0.92 in Triton X-100-induced hyperlipidaemic rats ($p<0.0001$). On the other hand, EA SN100 and EA SN200 treatment significantly reduced VLDL level to 32.50 ± 0.59 and 30.3 ± 0.48, respectively, compared to Triton X- 100 induced hyperlipidaemic rat ($p<0.001$).

4.4 Histopathology Analysis of Heart and Liver Tissue

4.4.1 Heart Tissue

Histopathological study of the heart stained with Haematoxylin and Eosin (H and E) in the control rat group (A) showed normal histological architectural appearance of cardiac myocytes in the cardiac muscle (→). Group B showed areas of significant damage with degenerated cardiac myocytes with vacuolated, dilated, congested blood capillaries, including areas of haemorrhage in between the cardiac muscle and inflammatory cellular infiltration (→). Group C rats showed mild to moderate cardiac muscle degeneration (→) with ruptured muscle fibres, vacuolated sarcoplasm and cellular infiltration (→). Group D rats showed protection of cardiac myocytes with notably improved ruptured muscle fibres appearing closer to normal tissue. (→). Group E rats showed protection of cardiac myocytes with improved cardiac muscle architecture appearing closer to normal tissue. (→). Finally, Group F showed restoration of cardiac muscles with normal architectural appearance of cardiac myocytes (→) (Figure 6).

Histopathological section in the heart of rats stained with Masson's trichrome stain in the control Group rats (A) showed normal collagen fibres and cardiac muscle. In Groups B and C, increased deposition of collagen fibre was seen. And in Groups D, E, and F decrease in collagen fibre formation (Figure 7).

4.4.2 Liver Tissue

Histopathology of rat liver using H and E stain in Group A showed normal hepatic lobules with a centrally located central vein and peripherally located portal triad with prominent round nuclei and eosinophilic cytoplasm arranged in plates with separate hepatic sinusoids. The portal triad of the hepatic artery, portal vein, and bile duct is normal. In Group B, massive fatty change and centrilobular necrosis with mononuclear cells infiltration, hypertrophy around central veins and in portal areas and macrovesicular steatosis were seen. Group C rats presented moderate fatty change and centrilobular necrosis with mononuclear cell

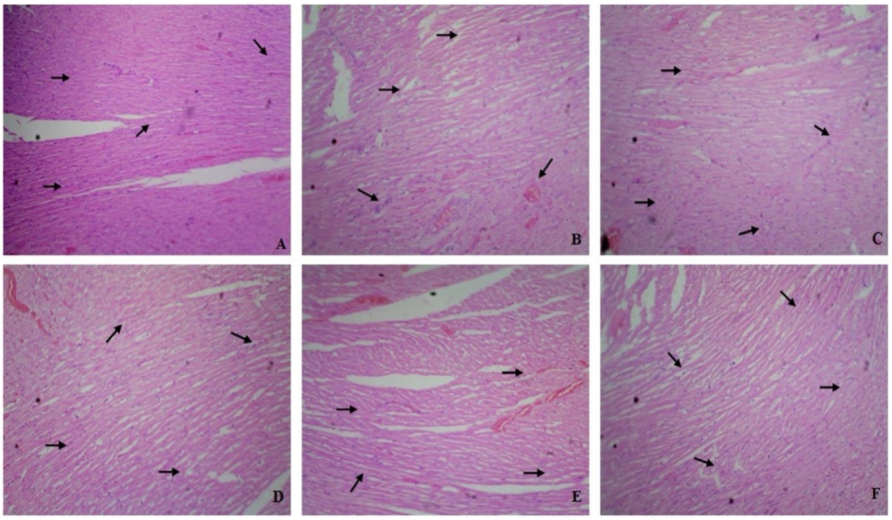


Figure 6. H and E staining of heart tissue. A: Control group; B: Negative control (TRITON X- 100); C:TRITON X- 100+EA SN100; D:TRITON X- 100+ EA SN200; E: TRITON X- 100+ EA SN300; F: TRITON X- 100+ ATV.

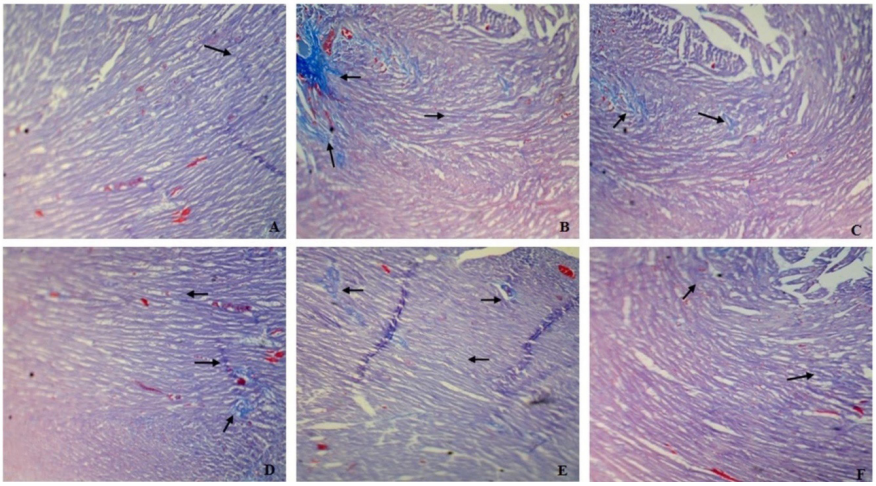


Figure 7. Masson's trichome staining of heart tissue. A: Control group; B: Negative control (TRITON X- 100); C:TRITON X- 100+EA SN100; D:TRITON X- 100+ EA SN200; E: TRITON X- 100+ EA SN300; F: TRITON X- 100+ AVS.

infiltration around central veins, dilatation of the sinusoidal space with minimal hypertrophy. Group D rats presented a reduction in fatty change, cellular hypertrophy, sinusoidal space and inflammatory cell infiltration around the central and portal areas with regeneration of hepatocytes. The liver of Group E treated rats exhibited clear hepatic tissue regeneration, exhibiting normal characteristic features comparable to the control group. And finally, Group F-treated rats showed regular tissue architecture features comparable to the control group (Figure 8).

As shown in Figure 9, no collagen fibre deposition was observed in Group A and F rats. In Groups B and C, rats, substantial collagen fibre deposition was seen. In Groups D and E, treated rats, moderate to minimal collagen fibre deposition was observed.

5. Discussion

The whole plant of *S. nigrum* was analysed for its anti-hyperlipidemic effects on Wistar albino rats with hyperlipidemia induced by Triton X- 100 X. The plant was extracted using various solvents, with the ethyl acetate extract chosen for further analysis due to its rich content of flavonoids, alkaloids, glycosides, protein, and carbohydrates. GCMS analysis of this extract identified

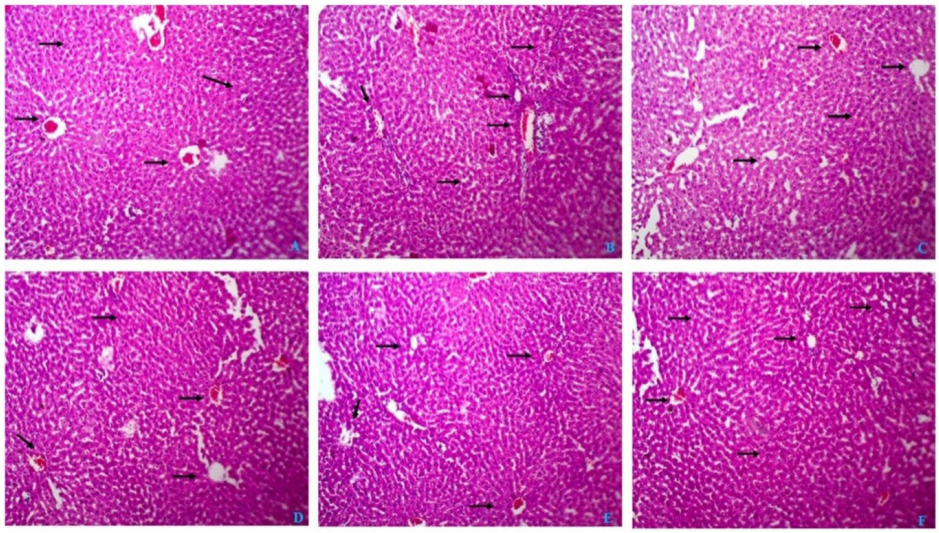


Figure 8. H and E staining of Liver tissue. A: Control group; B: Negative control (TRITON X- 100); C:TRITON X- 100+EA SN100; D:TRITON X- 100+ EA SN200; E: TRITON X- 100+ EA SN300; F: TRITON X- 100+ AVS.

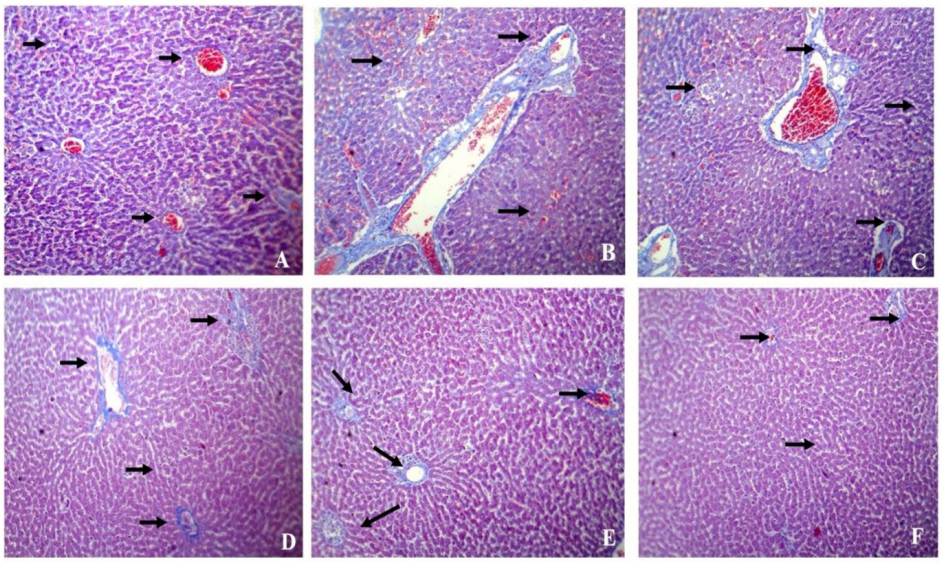


Figure 9. Masson's trichome staining of Liver tissue. A: Control group; B: Negative control (TRITON X- 100); C:TRITON X- 100+EA SN100; D:TRITON X- 100+ EA SN200; E: TRITON X- 100+ EA SN300; F: TRITON X- 100+ AVS.

10 compounds, including the biologically active compound, phytol[22]. In our GC-MS study, we detected a major peak (70.64%) for "Ethane, 1-chloro-1-fluoro-", and this molecule is not recognised as a plant secondary metabolite in general. In the process of preparing samples for analysis, the use of organic solvents for extraction is a standard practice. These solvents have the potential to chemically interact with different analytes. Moreover, any impurities present in the solvents could lead to the formation of artefacts. Functional groups like hydroxyl, aldehyde, keto, carboxyl, ester, and amine are especially prone to participating in artefact formation. During the preanalytical stages of sample preparation, common reactions that might occur include oxidation, esterification, hydrolysis, and glycolysis[23]. One drawback of this study is that we do not include a blank run that would have been informative with regard to the exogenous nature of this peak.

The extract then underwent *in-silico* evaluation through molecular docking and ADMET analysis. Molecular docking was performed on PDB1D-1HWI, a complex of human HMG-CoA reductase's

catalytic portion with Fluvastatin[24]. HMG-CoA reductase catalyses the rate-limiting step in cholesterol synthesis and is a target for inhibitors used to treat hypercholesterolemia[25]. Molecular docking simulates the physical interaction between a ligand and a protein receptor, producing a docking score that estimates binding strength and a docking pose showing the ligand's predicted 3D configuration in the protein's binding pocket[26]. A more negative score indicates stronger binding, while a less negative or positive score suggests weaker or no binding[25]. Of the identified constituents, seven showed negative scores, with Phytol and Cyclopentanemethanol demonstrating stability comparable to Fluvastatin, indicating significant binding interaction. Gibbs free energy (ΔG binding) determines the stability of ligand-receptor conformations. Lower free energy indicates a more stable molecule and a spontaneous reaction, aligning with the law of thermodynamic balance. More negative free energy suggests a spontaneous reaction and quicker formation of stable conformations[26]. The identified compounds showed DG bind values ranging from -11.89 to -44.78, with Phytol demonstrating a value similar to the standard Fluvastatin. Subsequently, ADMET analysis was conducted, and the results were evaluated according to Lipinski's rule of five. This rule is a computational and experimental approach for estimating solubility, membrane permeability, and efficacy in drug development[27]. The rule of five criteria suggests that suboptimal oral bioavailability is more probable when: (i) the atom-based calculated Log P (ALogP) exceeds 5, (ii) there are over 5 hydrogen-bond donors, (iii) there are more than 5 × 2 or 10 hydrogen-bond acceptors, and (iv) the molecular weight surpasses 5 × 100 or 500[28]. Lipinski's rule of five indicates potential bioavailability issues if two or more properties are violated[29]. In this study, none of the identified compounds violated more than one rule according to the rule of five criteria, indicating no bioavailability concerns. The toxicity of these compounds was assessed using ProTox-II 3.0, revealing that most fell into classes IV, V, and VI (where class IV is harmful if swallowed ($300 < LD50 \leq 2000$), class V may be harmful if swallowed ($2000 < LD50 \leq 5000$), and Class VI is non-toxic ($LD50 > 5000$))[30]. Based on previous research, three doses (100, 200, and 300 mg/kg BW) were chosen for the *in vivo* anti-hyperlipidemic study. Triton X- 100 X-induced hyperlipidemia model was employed to evaluate *the in vivo* anti-hyperlipidemic activity of the extract. Triton X- 100 X-100-induced hyperlipidemia is a widely recognised model for inducing cholesterol-induced hyperlipidemia. Triton X- 100 X-100, a non-ionic surfactant, enhances hepatic cholesterol synthesis and increases intestinal lipid absorption through emulsification. It inhibits lipoprotein lipase activity and prevents the uptake of lipoproteins from circulation by extrahepatic tissues, resulting in elevated blood lipid levels[31]. The administration of Triton X- 100 X led to increases in body weight, glucose, TGs, Cholesterol, LDL, VLDL, and a decrease in HDL. Treatment with the Ethyl acetate fraction of *S. nigrum*, particularly at doses of 200 and 300 mg/kg, normalised these parameters.

A previous study indicated that elevated blood glucose levels were positively correlated with high TG and TC[32]. Clinical research has shown that increased cholesterol levels lead to glucose tolerance deterioration, and a high TC to HDL-C ratio can predict type 2 diabetes[33]. Consequently, glucose levels in hyperlipidemic rats were also measured, and the extract demonstrated the ability to lower blood glucose in these rats. The lipid-lowering activity of *S. nigrum* may be attributed to its phytol content. Phytol is believed to possess significant anti-dyslipidemic properties through PPAR-α activation in the liver[34]. Phytol exerts insulin-sensitising and anti-diabetic effects, partly through nuclear receptor activation and RXR heterodimerization with PPARγ by its metabolite, phytanic acid. A study showed that phytol administration increases adipocyte numbers in inguinal subcutaneous white adipose tissue and improves glucose tolerance in mice fed a high-fat and high-fructose diet via activation of the phosphatidylinositol-4,5-bisphosphate 3-kinase (PI3K)/Akt signalling pathway. Furthermore, phytol administration in mice resulted in increased expression of genes associated with adipogenesis (C/EBPα and PPARγ) in inguinal subcutaneous white adipose tissue. This offers fresh perspectives on how phytol regulates fat cell formation and glucose absorption, suggesting its potential use as a nutritional supplement to address obesity and type 2 diabetes[22].

Our molecular docking analysis supports this hypothesis through a demonstration that phytol binds to the active site of HMG-CoA reductase (PDB 1HWK), forming hydrogen bonds with key residues

ARG590 and ASP690 (Table 3). These interactions are similar to those of Fluvastatin, and phytol might be directly inhibiting the enzyme, which is the rate-limiting cholesterol biosynthetic pathway.

Finally, histopathological analysis of heart and liver tissue in high-fat diet model rats revealed that higher doses of test extract 200 and 300 mg/kg restored the normal architecture of heart and liver and showed minimal to no deposition of collagen fibres.

Our findings are consistent with earlier research demonstrating the anti-hyperlipidemic effects of *S. nigrum* fruit[15], *S. nigrum* seed extract[35], and *S. nigrum* leaf extract[18]. Nevertheless, this study contributes novel insights into the potential of the whole plant as a source of bioactive compounds for managing hyperlipidemia.

6. Conclusion

The present study demonstrated the anti-hyperlipidemic properties of the ethyl acetate fraction of *S. nigrum* whole plant against Triton X- 100 induced hyperlipidemic rats. Biologically active phytochemicals such as flavonoids, glycosides, and alkaloids were present in the extract, and with GCMS analysis, molecular docking, and ADMET analysis, phytol was identified as a key bioactive constituent. *The S. nigrum* extract significantly reduced body weight, glucose, TC, TG, LDL, and VLDL, and improved HDL levels, demonstrating a lipid-lowering effect. These findings suggest that *S. nigrum*, specifically its phytol content, may serve as a potential herbal drug for managing hyperlipidemia and associated metabolic disorders.

7. References

1. Nelson RH. Hyperlipidemia as a risk factor for cardiovascular disease. Prim Care. 2013; 40(1):195-211. https://doi.org/10.1016/j.pop.2012.11.003
2. Sahathevan R. Dementia. In: Diet and Nutrition in Dementia and Cognitive Decline. London: Elsevier. 2015: pp. 187-198. https://doi.org/10.1016/B978-0-12-407824-6.00018-5
3. Ezeh KJ, Ezeudemba O. Hyperlipidemia: a review of the novel methods for the management of lipids. Cureus. 2021; 13(7):e16412. https://doi.org/10.7759/cureus.16412
4. Degrave V, Battisti M, Vega Joubert MB, Ingaramo P, Vaccarini C, *et al*. *Cannabis* oil: effects on cannabinoid-induced tetrad, blood pressure and metabolic parameters in female rats fed a sucrose-rich diet. Integr Food Nutr Metab. 2023; 10.
5. Giles LA. Hyperlipidemia prevention and management utilising lifestyle changes. J Midwifery Women's Health. 2024; 69(3):361-369. https://doi.org/10.1111/jmwh.13637
6. Alloubani A, Nimer R, Samara R. Relationship between hyperlipidemia, cardiovascular disease and stroke: A systematic review. Curr Cardiol Rev. 2021; 17(6):e051121189015. https://doi.org/10.2174/1573403X16999201210200342
7. Rauf A, Akram M, Anwar H, Daniyal M, Munir N, Bawazeer S, *et al*. Therapeutic potential of herbal medicine for the management of hyperlipidemia: latest updates. Environ Sci Pollut Res Int. 2022; 29(27):40281-40301. https://doi.org/10.1007/s11356-022-19733-7
8. Campisi A, Acquaviva R, Raciti G, Duro A, Rizzo M, Santagati NA. Antioxidant activities of *Solanum nigrum* L. leaf extracts determined in *in vitro* cellular models. Foods. 2019; 8(2):63. https://doi.org/10.3390/foods8020063
9. Sharma D, Joshi M, Apparsundaram S, Pathak S, Goyal S, Kumar S, *et al*. *Solanum nigrum* L. in COVID-19 and post-COVID complications: a propitious candidate. Mol Cell Biochem. 2023; 478(8):2221-2240. https://doi.org/10.1007/s11010-022-04654-3
10. Zhang H, Lv JL, Zheng QS, Li J. Active components of *Solanum nigrum* and their antitumor effects: a literature review. Front Oncol. 2023; 13:1329957. https://doi.org/10.3389/fonc.2023.1329957
11. Kumar J, Kaur A, Narang P. Phytochemical screening and metal binding studies on floral extract of *Solanum nigrum*. Mater Today Proc. 2019; 26:3332-3336. https://doi.org/10.1016/j.matpr.2019.09.170
12. Jia CY, Li JY, Hao GF, Yang GF. A drug-likeness toolbox facilitates ADMET study in drug discovery. Drug Discov Today. 2020; 25(1):248-258. https://doi.org/10.1016/j.drudis.2019.10.014
13. Fan J, Fu A, Zhang L. Progress in molecular docking. Quant Biol. 2019; 7(2):83-89. https://doi.org/10.1007/s40484-019-0172-y
14. Dias R, de Azevedo WF Jr. Molecular docking algorithms. Curr Drug Targets. 2008; 9(12):1040-1047. https://doi.org/10.2174/138945008786949432
15. Arulmozhi V, Krishnaveni M, Karthishwaran K, Dhamodharan G, Mirunalini S. Antioxidant and antihyperlipidemic effect of *Solanum nigrum* fruit extract on the experimental model against chronic ethanol toxicity. Pharmacogn Mag. 2010; 6(21):42-50. https://doi.org/10.4103/0973-1296.59965
16. Nderitu KW, Mecha E, Nyachieo A. *Solanum nigrum* show anti-obesity effects on high-fat diet-fed Sprague Dawley rats in a randomised study. Sci Afr. 2023; 20:e01713. https://doi.org/10.1016/j.sciaf.2023.e01713

17. Livingston R NR, Nair AR, Senthilpandian S, Ravi V. Hypolipidemic action of rutin on Triton X-100 WR-1339 induced hyperlipidemia in rats. J Pre Clin Clin Res. 2021; 15(2):51-55. https://doi.org/10.26444/jpccr/136231
18. Bouhlali EDT, Hmidani A, Bourkhis B, Moussafir Z, Filali-Zegzouti Y, Alem C. Date (*Phoenix dactylifera* L.) fruits as a potential lipid-lowering therapy: effect on high-fat diet and Triton X-100-WR-1339-induced hyperlipidemic rats. Drugs Drug Candidates. 2023; 2(2):422-32. https://doi.org/10.3390/ddc2020021
19. Soltan OIA, Gazwi HSS, Ragab AE, Mahmoud ME, Fudllalah FMN, Alqahtani MM, *et al*. Antihyperlipidemic effect of bread fortified with potato peel powder against Triton X-100 X-100-induced hyperlipidemia in male albino rats. J Funct Foods. 2023; 108:105725. https://doi.org/10.1016/j.jff.2023.105725
20. Islam MT, Ali ES, Uddin SJ, Shaw S, Islam MA, Ahmed MI, *et al*. Phytol: a review of biomedical activities. Food Chem Toxicol. 2018; 121:82-94. https://doi.org/10.1016/j.fct.2018.08.032
21. RCSB Protein Data Bank. 1HWI: HMG-CoA reductase [Internet]. 2001 [cited 2024 Jan 15]. Available from: https://www.rcsb.org/structure/1HWI
22. Istvan ES. Structural mechanism for statin inhibition of HMG-CoA reductase. Science. 2001; 292(5519):1160-4. https://doi.org/10.1126/science.1059344
23. Verpoorte R, Kim HK, Choi YH. Trivialities in metabolomics: Artefacts in extraction and analysis. Front Mol Biosci. 2022; 9:972190. https://doi.org/10.3389/fmolb.2022.972190
24. QIAGEN. Docking algorithms. In: CLC Drug Discovery Workbench Manual [Internet]. Aarhus (Denmark): QIAGEN; 2021 [cited 2024 Jan 15]. Available from: https://resources.qiagenbioinformatics.com/manuals/clcdrugdiscoveryworkbench/150/_docking_algorithms.html
25. Ojo OA, Adegboyega AE, Johnson GI, Umedum NL, Onuh K, Adeduro MN, *et al*. Deciphering the interactions of compounds from *Allium sativum* targeted towards identification of novel PTP 1B inhibitors in diabetes treatment: a computational approach. Inform Med Unlocked. 2021; 26:100719. https://doi.org/10.1016/j.imu.2021.100719
26. Malau ND, Azzahra SF. Molecular docking studies of potential quercetin 3,4'-dimethyl ether 7-alpha-L-arabinofuranosyl-(1-6)-glucoside as an inhibitor of malaria. J Phys Conf Ser. 2020; 1428:012057. https://doi.org/10.1088/1742-6596/1428/1/012057
27. Roskoski R Jr. Properties of FDA-approved small molecule protein kinase inhibitors: A 2024 update. Pharmacol Res. 2024; 200:107059. https://doi.org/10.1016/j.phrs.2024.107059
28. Roskoski R Jr. Rule of five violations among the FDA-approved small molecule protein kinase inhibitors. Pharmacol Res. 2023; 191:106774. https://doi.org/10.1016/j.phrs.2023.106774
29. Kumar DT, Shree Devi MS, Udhaya Kumar S, Sherlin A, Mathew A, Lakshmipriya M, *et al.* Understanding the activating mechanism of the immune system against COVID-19 by Traditional Indian Medicine: Network pharmacology approach. Adv Protein Chem Struct Biol. 2022; 129:1-24.
30. ProTox 3.0 - Prediction of Toxicity of Chemicals [Internet]. Berlin: Charité-Universitätsmedizin; 2023 [cited 2024 Jan 15]. Available from: https://tox.charite.de/protox3/
31. Parwin A, Najmi AK, Ismail MV, Kaundal M, Akhtar M. Protective effects of alendronate in Triton X-100 X-100-induced hyperlipidemia in rats. Turk J Gastroenterol. 2019; 30(6):557-564. https://doi.org/10.5152/tjg.2019.18076
32. Wang L, Yan N, Zhang M, Pan R, Dang Y, Niu Y. The association between blood glucose levels and lipids or lipid ratios in type 2 diabetes patients: A cross-sectional study. Front Endocrinol (Lausanne). 2022; 13:969080. https://doi.org/10.3389/fendo.2022.969080
33. Rhee EJ, Han K, Ko SH, Ko KS, Lee WY. Increased risk for diabetes development in subjects with large variation in total cholesterol levels in 2,827,950 Koreans: A nationwide population-based study. PLoS One. 2017; 12(5):e0176615. https://doi.org/10.1371/journal.pone.0176615
34. Singh SP, Sashidhara KV. Lipid-lowering agents of natural origin: An account of some promising chemotypes. Eur J Med Chem. 2017; 140:331-348. https://doi.org/10.1016/j.ejmech.2017.09.020
35. Sharma BK, Iyer D, Patil UK. Bioactivity guided fractionation in experimentally induced hyperlipidemia in rats and characterisation of phytoconstituent from *Solanum nigrum*. J Herbs Spices Med Plants. 2012; 18(3):257-267. https://doi.org/10.1080/10496475.2012.688933

Author Contributions

V.M., S.Z.B., A.K.U., R.J., F.S., T.S., M.J.S., and B.T. conceived the study, performed the extraction, GCMS, in vivo animal experiments, biochemical estimations, histopathology, and drafted the manuscript. S.A.A., A.K., and A.R.K. (Malaysiabased) conducted the in silico docking, ADMET analysis, statistical validation, and revised the manuscript. B.T. supervised the project. All authors have read and agreed to the published version of the manuscript.